THE JOURNAL OF BIOLOGICAL CHEMISTRY VOL. 282, NO. 46, pp. 33795–33804, November 16, 2007

Differences in the Single-stranded DNA Binding Activities of MCM2–7 and MCM467

*MCM2 AND MCM5 DEFINE A SLOW ATP-DEPENDENT STEP**

Received for publication, May 9, 2007, and in revised form, August 29, 2007 Published, JBC Papers in Press, September 25, 2007, DOI 10.1074/jbc.M703824200

Matthew L. Bochman and Anthony Schwacha[1]

From the Department of Biological Sciences, University of Pittsburgh, Pittsburgh, Pennsylvania 15260

The MCM2–7 complex, a hexamer containing six distinct and essential subunits, is postulated to be the eukaryotic replicative DNA helicase. Although all six subunits function at the replication fork, only a specific subcomplex consisting of the MCM4, 6, and 7 subunits (MCM467) and not the MCM2–7 complex exhibits DNA helicase activity *in vitro*. To understand why MCM2–7 lacks helicase activity and to address the possible function of the MCM2, 3, and 5 subunits, we have compared the biochemical properties of the *Saccharomyces cerevisiae* MCM2–7 and MCM467 complexes. We demonstrate that both complexes are toroidal and possess a similar ATP-dependent single-stranded DNA (ssDNA) binding activity, indicating that the lack of helicase activity by MCM2–7 is not due to ineffective ssDNA binding. We identify two important differences between them. MCM467 binds dsDNA better than MCM2–7. In addition, we find that the rate of MCM2–7/ssDNA association is slow compared with MCM467; the association rate can be dramatically increased either by preincubation with ATP or by inclusion of mutations that ablate the MCM2/5 active site. We propose that the DNA binding differences between MCM2–7 and MCM467 correspond to a conformational change at the MCM2/5 active site with putative regulatory significance.

Cellular DNA is double-stranded, yet during DNA replication it must be separated into component single strands. Although DNA polymerases require a single-stranded DNA (ssDNA)[2] template for activity, they have little or no intrinsic ability to unwind double-stranded DNA (dsDNA; reviewed in Ref. 1). DNA unwinding requires an ATP-dependent molecular motor termed the replicative helicase (reviewed in Ref. 2). In both prokaryotes and eukaryotes, the loading and activation of this helicase is a central and limiting event during DNA replication. Initiation culminates in replicative helicase loading, whereas the start of elongation requires extensive separation of duplex DNA by the helicase (reviewed in Refs. 3 and 4). Despite the critical importance of the replicative helicase, both its exact identity and mechanism remain controversial in eukaryotes.

Numerous studies implicate the minichromosome maintenance proteins (MCMs) as the replicative helicase. The MCMs are evolutionarily conserved from archaea to eukaryotes, with the archaea usually having a single MCM gene (5) and eukaryotes having six distinct and essential MCM genes (reviewed in Ref. 6). Each MCM protein (numbered 2–7) is an AAA^+ ATPase, whose members include DNA helicases such as SV40 large T antigen and the papilloma virus E1 protein (7). Similar to prokaryotic replicative helicases (reviewed in Ref. 8), the six MCM subunits are both physically present in initiation and elongation complexes and functionally essential for both phases of DNA replication, evidence strongly suggesting that all six MCM subunits unwind DNA at the replication fork (reviewed in Ref. 3).

Despite *in vivo* similarities to other replicative helicases, biochemical examination of the MCM complex has provided confounding results. Whereas the archaeal MCM proteins have robust helicase activity (9–12), a hexamer containing the six eukaryotic MCM subunits (MCM2–7; MCM2,3,4,5,6,7 hexamer) lacks this activity (13–17). In contrast, a hexameric subcomplex that specifically contains MCM4, 6, and 7 (MCM467) possesses a weak helicase activity (13, 15, 18).

Despite the apparent dispensability of the MCM2, 3, and 5 subunits for *in vitro* helicase activity, their ATP active sites are essential *in vivo*. Mutational analysis of the Walker A ATP-binding motif indicates that all six MCM subunits require this motif for both viability and S phase progression (17, 19). *In vitro* analysis of the corresponding MCM2–7 mutant complexes, however, indicates that the six MCM subunits fall into two functionally distinct subgroups (17). The Walker A motif in the MCM4, 6, and 7 subunits is essential for ATPase activity, whereas the ATP-binding motifs of the MCM2, 3 and 5 subunits contribute little to steady-state ATP hydrolysis hydrolysis (17). The discrepancy between the *in vivo* involvement of all six subunits in DNA replication and the *in vitro* participation of only a specific subgroup of MCM subunits in DNA unwinding remains unexplained. Recently, MCM2–7 has been isolated *in vivo* as part of a larger macromolecular complex having ATP-dependent helicase activity; this complex additionally contains the essential GINS complex and CDC45, suggesting that these factors are activators of MCM helicase activity (20).

Although MCM467 has been extensively characterized biochemically, little work has been done with the MCM2–7 heterohexamer. To determine why the MCM2–7 complex lacks

* This work was supported by Grant RSG-05-113-01-CCG from the American Cancer Society (to A. S.). The costs of publication of this article were defrayed in part by the payment of page charges. This article must therefore be hereby marked "*advertisement*" in accordance with 18 U.S.C. Section 1734 solely to indicate this fact.

S The on-line version of this article (available at http://www.jbc.org) contains supplemental Tables S1 and S2 and supplemental Figs. S1–S3.

[1] To whom correspondence should be addressed: 4249 Fifth Ave., 560 Crawford Hall, Pittsburgh, PA 15260. Tel.: 412-624-4307; Fax: 412-624-4759; E-mail: schwacha@pitt.edu.

[2] The abbreviations used are: ssDNA, single-stranded DNA; dsDNA, double-stranded DNA; MCM, minichromosome maintenance protein; BSA, bovine serum albumin; ATPγS, adenosine 5′-*O*-(thiotriphosphate).

helicase activity, as well as to elucidate the function of the MCM2, 3, and 5 subunits, we have undertaken a comparative analysis of the ssDNA binding activity of the *Saccharomyces cerevisiae* MCM2–7 and MCM467 complexes. Our studies with MCM2–7 indicate that its lack of DNA helicase activity is not due to an inability to bind ssDNA, because both complexes have similar ssDNA binding affinities. However, we find an important difference between these complexes in ssDNA association rates. Because these two complexes differ in subunit composition (*i.e.* MCM2, 3, and 5), the functional difference between them suggests that the additional subunits regulate the manner in which the MCM2–7 complex interacts with DNA.

EXPERIMENTAL PROCEDURES

Buffers and Reagents—Buffers used include B1 (5 mM Tris-HCl, pH 7.5, 0.5 mM EDTA, 1 M sodium chloride, 100 μg/ml bovine serum albumin (BSA)), B2 (25 mM potassium-HEPES, pH 7.4, 50 mM potassium chloride, 10 mM magnesium acetate, 50 μM zinc acetate, 100 μM EDTA, 10% glycerol, 0.02% Nonidet P-40, 1 mM dithiothreitol), B3 (25 mM potassium-HEPES, pH 7.4, 10 mM potassium chloride, 5 mM magnesium acetate, 50 μM zinc acetate, 100 μM EDTA, 10% glycerol), and B4 (25 mM sodium-HEPES, pH 7.4, 50 mM sodium chloride, 10 mM magnesium acetate, 50 μM zinc acetate, 100 μM EDTA, 10% glycerol, 0.02% (v/v) Nonidet P-40, 1 mM dithiothreitol, 100 μg/ml BSA). 1× TBE contains 90 mM Tris base, 90 mM boric acid, and 2 mM EDTA, adjusted to pH 8.0 with HCl. Radiolabeled nucleotides were purchased from PerkinElmer Life Sciences or MP Biomedical, and unlabeled ATP was obtained from GE Healthcare. Oligonucleotides were purchased from Integrated DNA Technologies (Coralville, IA; supplemental Table S1). Polynucleotide substrates were from GE Healthcare or Sigma. Nucleotide and DNA concentrations were calculated from absorbance at 260 nm. All other reagents were of the highest available purity.

Proteins and Purification—Hexameric MCM2–7 and MCM467 complexes were expressed and purified as described (17). The presence of individual MCM subunits were either directly visualized following separation by SDS-PAGE (for MCM6, 3, and 5) or using Western blot analysis with subunit-specific antibodies (Santa Cruz anti-MCM2 (sc-6680) and anti-MCM7 (sc-6688) and anti-MCM4 monoclonal antibody (AS6.1).[3] MCM subcomplexes were purified similar to the hexameric complexes and were made using specific mixtures of recombinant baculoviruses that each encode the desired MCM subunits, with one MCM subunit containing a C-terminal His tag to facilitate metal chelate chromatography. SV40 large T-antigen was expressed in insect cells and purified as a C-terminal His-tagged protein; details are available upon request. All of the proteins were dialyzed against B2 buffer containing 100 mM potassium chloride and protease inhibitors. Protein concentrations were quantified using a Fuji FLA-5100 laser imager on SDS-PAGE-separated protein bands stained with Sypro orange (Molecular Probes, Eugene OR) using known amounts of BSA as a standard; protein concentrations unless otherwise noted are in pmol or nM of hexamer. MCM genes containing the Walker A (KA) or arginine finger (RA) alleles were completely sequenced to verify the constructs and used to make MCM complexes in a manner identical to the wild type complexes (17).

Helicase Assay—The helicase assay was performed essentially as described (21). Briefly, synthetic replication forks were prepared by annealing an equimolar mixture of oligonucleotides 233 and 235 (supplemental Table S1) and then filling in the resulting 5′ overhang with [^{32}P]dATP in the presence of the other dNTPs using reverse transcriptase. The resulting forks were then gel-purified from an 8% native acrylamide gel following electroelution into a dialysis membrane, ethanol-precipitated, and resuspended to a concentration of ~1 μM in 1× TE. The reactions were incubated for 1 h at 37 °C, stopped by the addition of unlabeled oligonucleotide 235 to 20 nM, proteinase K to 4 mg/ml, SDS to 0.4%, and a one-tenth volume of 10 × stop-load (25% w/v Ficoll (type 400), 100 mM EDTA, 0.1% SDS, 0.25% bromphenol blue, and 0.25% xylene cyanol) and heated at 50 °C for 20 min. The samples were then separated on an 8% polyacrylamide gel at room temperature. The gel was subsequently dried, and the results were imaged and quantified using Fuji FLA-5100 phosphorimaging and Image Gauge software.

Double Filter Binding Assay—The DNA double filter binding assay was based on the work of Wong and Lohman (22). Nitrocellulose (BA85; Schleicher & Schuell) and DEAE-cellulose (DE81, Whatman) filters were prepared as described. The ssDNA substrates were 5′ radiolabeled using T4 polynucleotide kinase and [γ-^{32}P]ATP. The dsDNA substrate was made by annealing an equimolar amount of nucleotide 510 to oligonucleotide 806 (supplemental Table S1), which was extended using exo$^-$ Klenow fragment (New England Biolabs) in the presence of unlabeled dNTPs spiked with [α-^{32}P]dATP. Standard ssDNA binding reactions contained 4 nM of unlabeled nucleotide substrate spiked with a small quantity of ^{32}P labeled substrate, 120 nM MCM hexamer, 5 mM of either ATP or ATPγS, 5 mM β-glycerophosphate all in 1× buffer B2 with a final volume of 12.5 μl. The reactions were incubated for 30 min (unless otherwise indicated) at 30 °C and then spotted onto a filter stack and quickly washed with an additional 500 μl of B2. After filtration using a FH 225V Filter Manifold (GE Healthcare), the nitrocellulose and DEAE membranes were separated and quantified by scintillation counting. The amount of DNA bound was calculated using Equation 1,

$$\mathrm{DNA_{bound}} = \frac{C_{NC}}{C_{NC} + C_{DEAE}} \qquad \text{(Eq. 1)}$$

where C_{NC} and C_{DEAE} are the radioactive counts retained on the nitrocellulose and DEAE membranes, respectively. The data points represent the averages of ≥3 repeats of the same experiment, and the *error bars* correspond to the standard deviations. The association kinetics were plotted as described (23, 24) using Equation 2,

$$\left[\frac{1}{(R) - (O)}\right] \ln\left[\frac{(O)[(R) - (RO)]}{(R)[(O) - (RO)]}\right] = k_a t \qquad \text{(Eq. 2)}$$

where (R) and (O) are the total concentrations of MCM and ssDNA, respectively, and (RO) is the concentration of the MCM·ssDNA complex at time t.

Magnetic Bead Binding Assay—Streptavidin-coated Dynabeads (M280, Dynal Biotech ASA, Oslo, Norway) were pre-

[3] A. Schwacha and S. Bell, unpublished observations.

pared per the manufacturer's instructions. Biotinylated oligonucleotide 455 (supplemental Table S1) was immobilized on the beads in buffer B1 for ≥30 min at 22 °C, and the oligo-bound beads were separated by a magnet and washed to remove unbound oligonucleotide. Experiments using a radiolabeled oligonucleotide indicate that about 90 pmol of oligonucleotide were bound per 1 mg of beads. For each binding experiment, 20 μl of beads were used. Following equilibration in buffer B3, the beads were resuspended in 25-μl reactions containing B3, protein, and nucleotide as indicated and incubated for ≥30 min at 22 °C. The beads were separated from unbound reaction components with a magnet, washed once with 50 μl of either B3 or B3 supplemented with additional sodium chloride as indicated, resuspended in 10 μl B3, and analyzed by SDS-PAGE and Sypro orange staining as described above.

Electrophoretic Mobility Shift Assay—Binding reactions contained protein as indicated, 4 nM of radiolabeled oligonucleotide 3 (supplemental Table S1), and 5 mM ATPγS. The reactions were incubated for 30 min at 30 °C and then separated by electrophoresis at 4 °C through a prechilled 3.5% native polyacrylamide gel (30:1 acrylamide:bis containing 0.5× TBE, 5% glycerol, 67 μg/ml acetylated BSA, and 10 mM magnesium acetate) using 0.5× TBE running buffer supplemented with 80 μg/ml BSA and 10 mM magnesium acetate at 15 volts/cm. Protein·ssDNA complexes were imaged and quantified using Fuji FLA-5100 phosphorimaging.

RESULTS

MCM2–7 and MCM467 Form Toroidal Complexes of Differing Helicase Activity—Hexameric preparations of *S. cerevisiae* MCM2–7 and MCM467 were expressed in baculovirus-infected insect cells and purified to homogeneity (supplemental Fig. S1). Gel filtration and co-immunoprecipitation of the final preparations demonstrated that the complexes retained their hexameric size as was observed previously (17), and these preparations contained approximately equal stoichiometry of the specified MCM subunits as determined by two-dimensional gel electrophoresis and quantitative Western blotting (supplemental Fig. S1). As described below, these preparations demonstrated an ATP-dependent ssDNA binding activity; the average specific activity of our preparations for this activity is ≥50% of total protein (supplemental Fig. S1).

Using transmission electron microscopy, the MCM2–7 and MCM467 preparations appear largely homogeneous (Fig. 1*A*), with many individual complexes having a diameter (top) and height (side) of ~145 Å and an apparent central cavity 25–30 Å wide. Examination of hundreds of complexes from both preparations demonstrates that 20–30% appear as ring-shaped structures, with about half containing six distinct lobes (Fig. 1*A*, *small insets*). Image reconstruction of the ring-shaped structures indicates that both complexes are of similar size and have pseudo 6-fold symmetry (Fig. 1*A*, *large insets*). These results are consistent with the published size and toroidal subunit organization of both eukaryotic MCM complexes (25–27), as well as the archaeal MCM complexes (9, 28–30).

Both the MCM467 and MCM2–7 preparations were tested for helicase activity. Although the MCM467 complex displays ATP-dependent helicase activity (Fig. 1*B*, *lanes 4–7*) similar to that of the SV40 large T antigen helicase (*lane 3*), MCM2–7

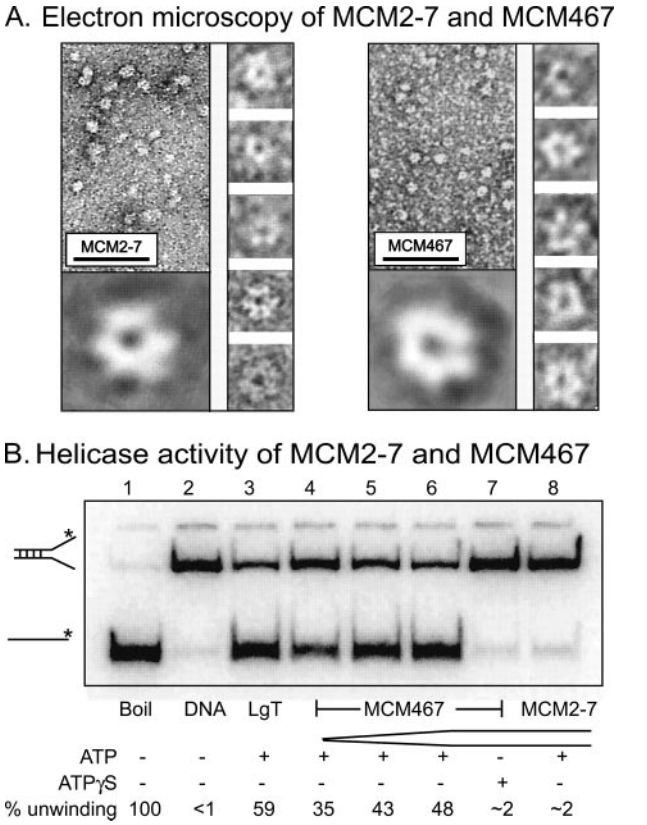

FIGURE 1. **Comparison of MCM2–7 and MCM467.** *A*, electron micrographs of both wide field and five individual hexamers of representative MCM2–7 (*left panel*) and MCM467 (*right panel*) preparations (supplemental materials). The *size bars* represent 100 nm (wide field) and 10 nm (individual hexamers), respectively. The large hexamer *inset* represents a composite of several dozen individual hexamers (supplemental materials). *B*, helicase assay. *Lane 1* shows dissociated ssDNA, and *lane 2* shows the position of the intact fork. *Lane 3* contains 1 pmol T-antigen monomer with ATP, and *lanes 4–6* contain 0.4, 0.8 and 1.6 pmol of MCM467 with ATP. *Lane 7* contains 1.6 pmol of MCM467 with ATPγS, and *lane 8* contains 1.6 pmol of MCM2–7 with ATP. The percentage of DNA substrate unwound is indicated.

displays no appreciable DNA unwinding (*lane 8*) and has an activity comparable with MCM467 in the presence of ATPγS (*lane 7*). The difference in helicase activity between these two complexes reconfirms previous results (13, 15–18, 31).

ATP-dependent ssDNA Binding Activity of the MCM Complexes—The ability of each MCM preparation to bind a short mixed sequence oligonucleotide (85 nt, oligonucleotide 510; supplemental Table S1) using a filter binding assay was examined. Both complexes demonstrate ATP-dependent ssDNA binding as a function of either MCM or ssDNA concentration (Fig. 2, *A* and *B*). Little ssDNA binding occurs in the absence of ATP (data not shown) or in the presence of GTP (Fig. 2*A*). This interaction requires ATP binding but not hydrolysis; the poorly hydrolyzable ATP analog ATPγS (17) stimulates the extent of ssDNA binding for both complexes relative to ATP (Fig. 2*A*). Further, this binding activity is MCM-dependent, because it is abolished upon preincubation of either the MCM2–7 or MCM467 complex with a monoclonal antibody that specifically binds the Walker B site in each MCM subunit (antibody AS1.1; data not shown (32)).[4] These data fit a

[4] A. Schwacha and J. Bowers, unpublished observations.

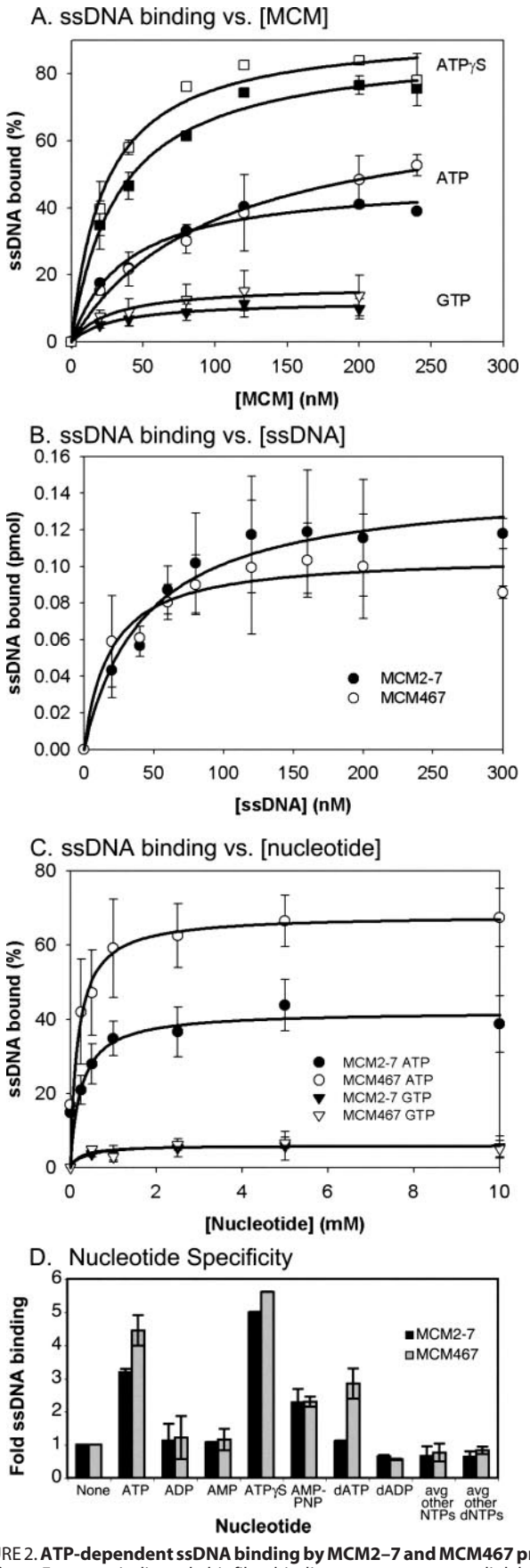

FIGURE 2. **ATP-dependent ssDNA binding by MCM2–7 and MCM467 preparations.** Except as indicated, this filter binding assay uses 4 nM radiolabeled oligonucleotide 510 (supplemental Table S1) in a 12.5-μl reaction volume with 5 mM ATP and 120 nM of either MCM2–7 or MCM467. *A*, MCM protein titrations. *Closed symbols*, MCM2–7; *open symbols*, MCM467. *B*, titration of ssDNA. Conditions were identical to those in *A* and used 5 mM ATP. *C*, ssDNA binding as a function of either [ATP] or [GTP]. *D*, MCM ssDNA binding requires adenosine triphosphates. The *bar graph* represents standard filter binding reactions that contain 5 mM of the indicated nucleoside. The values indicated are relative to the level of ssDNA binding in the absence of added nucleotide (*None*).

hyperbolic function, consistent with a homogeneous population of molecules demonstrating noncooperative binding. Repeats of this assay with shorter probes (oligonucleotides 3 (44 nt) and 775 (40 nt); supplemental Table S1) generate similar results (data not shown). MCM phosphorylation appears to have little effect on ssDNA binding. Neither treating the complexes with lambda phosphatase to remove phosphorylation that may occur during insect cell expression nor adding phosphates with a recombinant preparation of CDC28/CLB5 (a gift from S. P. Bell, Massachusetts Institute of Technology) appreciably alters ssDNA binding levels (data not shown).

From these graphs, an apparent K_d for ssDNA binding can be determined; using either ATP or ATPγS, both MCM complexes have a K_d of ~35 15 nM. The independent K_d values calculated from either the binding as a function of [MCM] (Fig. 2*A*) or [ssDNA] (Fig. 2*B*) are in good agreement (supplemental Table S2). These values are in the range of those previously observed for MCM467 (apparent K_d of ~2 nM using a 37-mer oligonucleotide (26)) and the archaeal MCM complex (apparent K_d of ~150–200 nM using a fork substrate (33)) and are typical of hexameric helicases (60 pM to 200 nM (2)).

ATP-dependent ssDNA binding was further examined as a function of nucleotide concentration (Fig. 2*C*). Both MCM complexes have similar ATP dependences (the $k_{½(ATP)}$ values for MCM2–7 and MCM467 being 248 152 and 177 82 μM, respectively) with maximal ssDNA binding coinciding with physiological ATP concentrations (~3 mM (34)). The nucleotide specificity of ssDNA binding by both MCM complexes was also tested (Fig. 2*D*). The triphosphate form of adenosine is needed to promote ssDNA binding, because neither ADP, AMP, dADP, nor any non-adenosine nucleotide support this activity (Fig. 2*D*).

The Identity of MCM Subunits within the MCM·ssDNA Complexes—The protein requirements for ssDNA binding were examined next. Filter binding experiments using various MCM subcomplexes demonstrated little or no ssDNA binding; however, when these subcomplexes were combined to generate either a MCM467 (MCM4/6 dimer + MCM7 monomer) or MCM2–7 (MCM2/4/6 trimer + MCM3/5/7 trimer) complex, high levels of ssDNA binding were recovered (data not shown and Fig. 3*A*). These results indicate that ssDNA binding is not an intrinsic property of any individual subunit but requires considerable oligomerization of MCM subunits. The only subcomplex that demonstrated substantial ssDNA binding was a MCM pentamer lacking MCM6 (Fig. 3*A*). This subcomplex is largely present as a variety of split ring structures rather than a closed toroid as visualized by electron microscopy (data not shown) and illustrates that although higher order MCM oligomerization is required for ssDNA binding, closure of the ring structure is not.

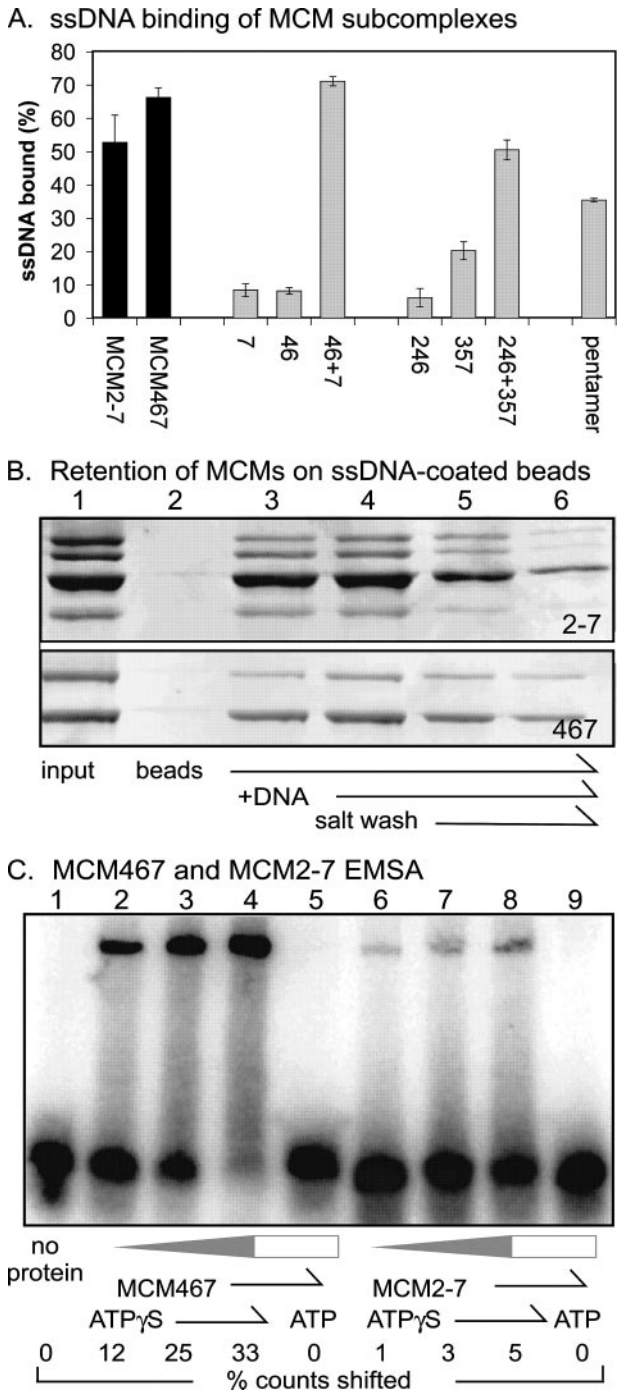

FIGURE 3. **MCM subunit involvement in ssDNA binding.** *A*, filter binding of 120 nM of the indicated MCM subcomplexes with ssDNA, 5 mM ATPγS, and 4 nM oligonucleotide 510 (supplemental Table S1). *B*, a magnetic bead binding assay containing biotinylated ssDNA. *Lane 1*, input protein (2.5 pmol) alone; *lane 2*, naked beads incubated with protein; *lane 3*, ssDNA-coated beads incubated with protein; *lanes 4–6*, ssDNA-coated beads incubated with protein and 5 mM ATP. The reactions in *lanes 1–4* were washed with buffer containing 50 mM NaCl; the sample in *lane 5* was washed with buffer containing 250 mM NaCl, and the sample in *lane 6* was washed with buffer containing 500 mM NaCl. Although the assay is ssDNA-dependent, it is not ATP-dependent. We speculate that the effective ssDNA concentration on the surface of the beads is sufficiently high to drive MCM binding even in the absence of ATP. *C*, electrophoretic mobility shift assay of MCM/ssDNA binding. The reactions contained radiolabeled oligonucleotide 3 (supplemental Table S1) and 5 mM ATP or ATPγS with increasing amounts of MCM protein (see "Materials and Methods" for details). *Lane 1*, no protein; *lanes 2–4*, 37.5, 75, 150 nM MCM467 with 5 mM ATPγS; *lane 5*, 150 nM MCM467 with 5 mM ATP; *lanes 6–8*, 37.5, 75, 150 nM MCM2–7 with 5 mM ATPγS; *lane 9*, 150 nM MCM2–7 with 5 mM ATP. The percentage of total counts shifted is noted.

To identify the MCM subunits that stably associate with ssDNA, binding experiments were performed using magnetic streptavidin beads coupled to biotinylated ssDNA (Fig. 3*B*). Following the addition of either the MCM2–7 or MCM467 complexes, the beads were washed in buffers of increasing salt concentration, and the proteins retained on the beads were analyzed by SDS-PAGE followed by either silver staining (Fig. 3*B*) or Western blotting to identify co-migrating MCM subunits (data not shown). In both cases, all input MCM subunits were retained on the beads in a ssDNA-dependent manner, strongly consistent with the notion that intact MCM hexamers bind ssDNA. Furthermore, these interactions are stable in moderate concentrations of salt as observed for MCM complexes on chromatin isolated during S phase (stable to 250 mM (35)), in contrast to the salt-sensitive chromatin binding observed during the G_1 phase (35, 36).

To examine the oligomeric state of the MCM·ssDNA complexes, an electrophoretic mobility shift assay was used (Fig. 3*C*). The ability of MCM complexes to bind ssDNA in this assay varies widely; several studies only observe a shift of MCM467 in the presence of a cross-linking agent (15, 26) or that the shift is inhibited in the archaeal MCMs by ATPγS (9). However, other studies with MCM467 have observed ATPγS-dependent mobility shifts (14, 18). Using the MCM467 complex and radiolabeled oligonucleotide #3 (44 nt), we observe nucleotide-dependent binding (using ATPγS); titrations with increasing amounts of MCM467 suggest a K_d of a magnitude similar to the K_d observed by filter binding (supplemental Table S2; ~40 nM). However, unlike the filter binding experiments, this activity is only supported by ATPγS but not ATP (Fig. 3*C*, *lane 5*). Only one shifted band was present throughout the range of the protein titration, suggesting that the MCM467·ssDNA complex represents a single, defined species, although we cannot rule out the possibility of different co-migrating MCM·ssDNA complexes. This conjecture is further supported by experiments using the longer oligonucleotide 510 (85 nt) as a probe; again only a single shifted species was observed over the range of MCM concentrations (data not shown).

In contrast, under identical assay conditions, the MCM2–7 complex demonstrates little or no electromobility shift (Fig. 3*C*, *lanes 6–8*, maximum shift = ~5%). These results suggest that even though the K_d values for these two complexes are similar as determined by filter binding, the MCM2–7 complex is more susceptible to dissociation from ssDNA under these conditions than the MCM467 complex.

Polynucleotide Substrate Requirements for MCM·DNA Binding—The sequence specificity of MCM·ssDNA binding was assayed using the ability of unlabeled polynucleotides to compete with radiolabeled ssDNA for binding. Prior to addition of MCM complexes, labeled oligonucleotide was mixed together with a 1-fold (not shown), 10-fold (not shown), or 100-fold (Fig. 4*A*) weight excess of the indicated DNA or RNA homopolymers; the observed competition was dosage-dependent and increased with higher competitor levels. In general, the MCM2–7 complex demonstrates a higher degree of sequence specificity than MCM467. As previously reported (13, 18), poly(dT) is the best competitor for MCM467; however, MCM2–7 demonstrates an even higher preference (about 2.5

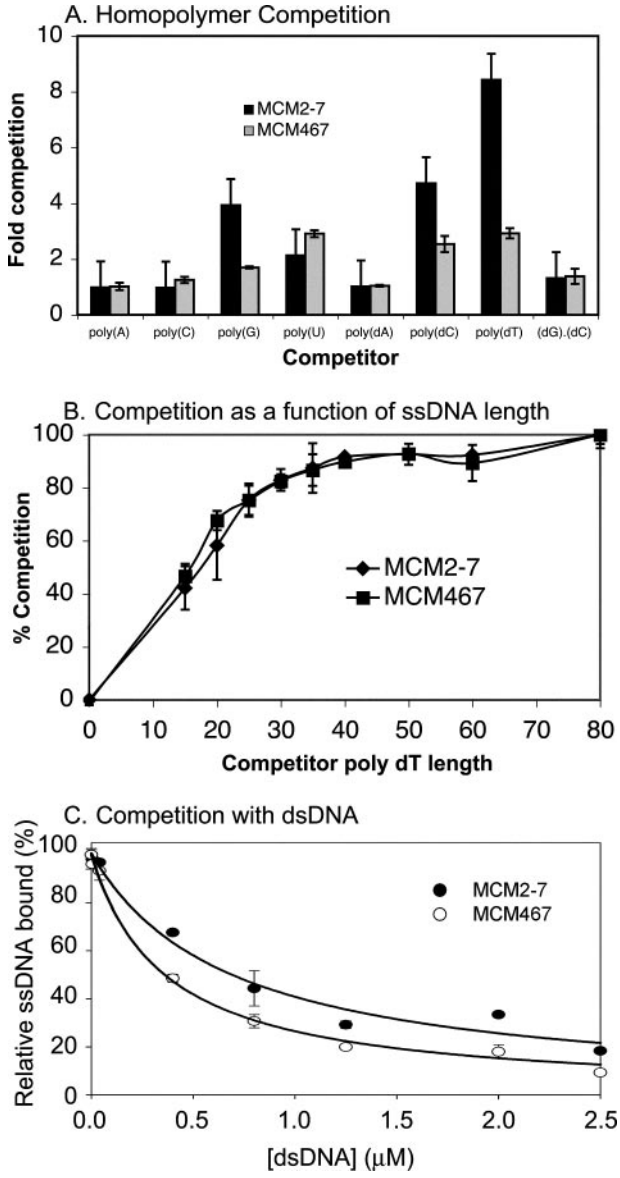

FIGURE 4. **Substrate requirements for MCM binding.** The reactions in *A* and *B* contained unlabeled competitor RNA or DNA with 120 nM MCM2–7 or MCM467, 5 mM ATPγS, and either 4 nM radiolabeled oligonucleotide 510 (*A*) or oligonucleotide 778 (*B*; supplemental Table S1). Competitor and radiolabeled ssDNA substrates were mixed prior to protein addition. *A*, competition of 100-fold weight excess of unlabeled ssRNA, ssDNA, and dsDNA homopolymers for either MCM2–7 or MCM467 binding to labeled oligonucleotide. The results were plotted as fold competition, where a 10-fold competition corresponds to a 90% reduction in MCM binding to the labeled oligonucleotide. *B*, the addition of 100-fold molar excess of unlabeled poly(dT) competitor ssDNA oligonucleotides of length 15, 20, 25, 30, 35, 40, 50, 60, or 80 nt to standard binding reactions containing radiolabeled poly(dT) 80mer. *C*, the indicated amount of unlabeled dsDNA substrate was added to standard ssDNA binding reactions (4 nM ^{32}P-labeled oligonucleotide 510, 120 nM MCM hexamer, 5 mM ATPγS, final volume of 12.5 μl). The reactions were incubated and filtered as described under "Double Filter Binding Assay." The data were normalized to the "no competitor" reaction and plotted as hyperbolic decay using nonlinear regression. The IC_{50} 683 78.6 nM and 360 26.5 nM for MCM2–7 and MCM467, respectively.

times better competition) for poly(dT) than MCM467. Similarly, poly(dC) competes for ssDNA binding with both MCM2–7 and MCM467, although not to as high a degree as poly(dT). In addition, polyribonucleotides are also capable of competing for binding, with poly(G) and poly(U) being the most effective. RNA binding by MCM467 has previously been shown (37).

The DNA length dependence of the MCM·ssDNA interaction was next tested (Fig. 3*B*). Competition experiments using unlabeled poly(dT) oligonucleotides of various defined lengths indicate that ssDNA of 15 nt is capable of competing, although maximum competition requires a length of ≥40 nt. The results were the same for both complexes and are similar to previous studies of ssDNA binding by MCM467 (between 37 and 50 nt (14, 15, 18, 26)). These experiments do not indicate the location of the ssDNA-binding site within either MCM complex. However, assuming an axial rise of ~3.5 Å/base for single-stranded poly(dT) (38), a 40-nt oligonucleotide corresponds to a length of 122.5–140 Å. This is similar to the observed length of the central channel (~145 Å; Fig. 1*C*), consistent with the likelihood that ssDNA binding occurs in this region.

The ability of the MCM2–7 and MCM467 complexes to bind blunt-ended dsDNA was also examined. Using a double-stranded form of our standard probe (85 bp, "Materials and Methods"), filter binding was performed as a function of MCM concentration (data not shown). The binding affinity of either complex for dsDNA was considerably less than for ssDNA, precluding a determining of a K_d by this approach. Like the ssDNA binding activity, dsDNA binding is ATP-dependent and is blocked by preincubation with antibody AS1.1 (data not shown). To obtain an estimate of K_d, a competition experiment was conducted to quantify the ability of dsDNA to compete for MCM ssDNA binding, yielding a K_d of ~5.60 μM for MCM2–7 and 2.12 μM for MCM467 (Fig. 4*C* and supplemental Table S2). MCM467·dsDNA binding has been previously observed for probes with 3′ ssDNA tails (21, 39), but we find that probes containing either a 10-nt 3′ or 5′ extension are bound similarly to the blunt-ended probe (data not shown).

MCM2–7 and MCM467 Associate Differently with ssDNA; MCM2–7 Has an Additional ATP-dependent Step—To further examine ssDNA binding by both complexes, the dissociation and association rates (k_d and $k_{a\,(apparent)}$, respectively) were measured. The observed dissociation for the two complexes was quite similar and slow (supplemental Fig. S2), with the MCM467 complex having a slightly slower k_d than the MCM2–7 complex. Interestingly, their apparent association rates were quite different (Fig. 5*A*). Using ATPγS, the MCM467 complex binds ssDNA quickly, with ~50% of total binding occurring in ~2.5 min; the MCM2–7 complex binds ssDNA very slowly, with 50% ssDNA binding occurring in ~12 min. Substituting ATP for ATPγS gave similar results (not shown).

The difference in the association rates between these two complexes was further investigated. We reasoned that the relatively slow association of the MCM2–7 complex with ssDNA could reflect one or more additional ATP-dependent steps by MCM2–7 prior to productive ssDNA binding. To test this hypothesis, both complexes were separately preincubated with ATPγS for 30 min, and then ssDNA was added. Although preincubation with nucleotide has little effect on the kinetics of MCM467 binding, nucleotide preincubation with MCM2–7 greatly accelerates its association rate to resemble that of MCM467 (Fig. 5*B*). Similar results were obtained using ATP (data not shown). These data demonstrate that the slow asso-

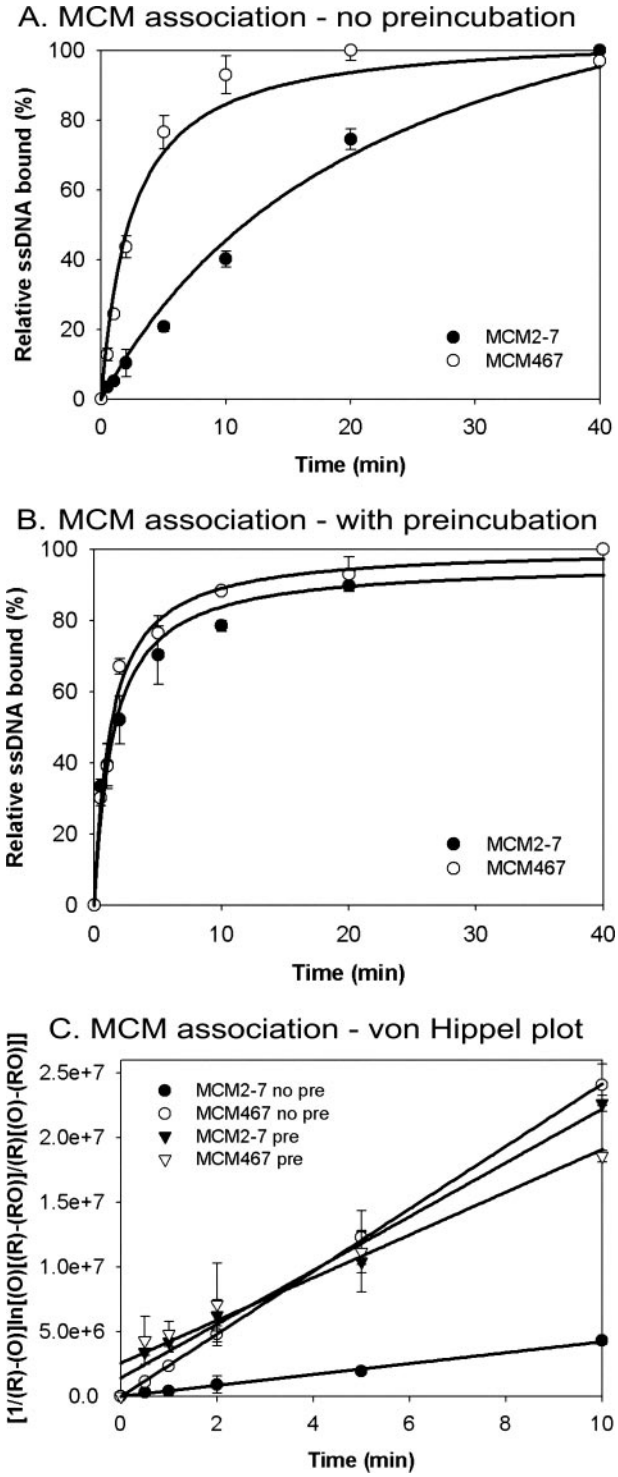

FIGURE 5. **Kinetics of MCM/ssDNA association.** *A*, association rates of MCM2–7 and MCM467. Standard binding reactions were scaled up 10-fold, MCMs were added at *t* 0, and 5-μl samples were withdrawn at the indicated times and analyzed by filter binding. The reactions contain 5 mM ATPγS, 4 nM radiolabeled oligonucleotide 510 (supplemental Table S1), and 120 nM MCM protein. *B*, effect of nucleotide preincubation on MCM·ssDNA association rates. Preparations of MCM2–7 or MCM467 were preincubated with ATPγS for 30 min at 30 °C prior to the addition of labeled oligonucleotide 510 at t 0. *C*, the data in *A* (*no pre*) and *B* (*pre*) were replotted in the manner of von Hippel (24); slope k_a.

ciation of MCM2–7 in the absence of ATP preincubation reflects an interaction between the MCM2–7 complex and ATP rather than slow ssDNA binding. To obtain association constants (supplemental Table S2), the results were replotted in the manner of von Hippel (Fig. 5*C* and Ref. 24).

It should be noted that even at the faster association rate, the ssDNA binding activity of the MCMs is considerably slower than would be anticipated for simple diffusion-limited bimolecular rates (10^7–10^8 M^{-1} s^{-1}) and is somewhat slower than what is commonly observed other hexameric helicases (2, 40). Because ssDNA binding likely occurs within the central channel of the complex, the relatively slow binding that is observed may correspond to specific ssDNA loading into the channel rather than simple binding *per se*.

The Involvement of MCM ATP Active Sites in ssDNA Binding—To determine which MCM ATP active sites contribute to ssDNA binding, we tested mutant MCM2–7 complexes containing alanine substitution mutations of the universally conserved lysine within the Walker A ATP-binding motif (the MCM KA mutants; Fig. 6*A*). These mutant complexes were expressed and purified as stable heterohexamers in a manner identical to the wild type complexes. We previously characterized such mutant complexes for their effects on steady-state ATP hydrolysis; inclusion of any one such mutant subunit in the context of the remaining five wild type subunits largely abolishes ATP hydrolysis of the entire heterohexamer (17).

Seven mutant MCM2–7 complexes were tested for ATP-dependent ssDNA binding. Six complexes contain a single indicated KA mutant subunit in the presence of five other wild type subunits; the seventh complex contains the KA mutation in all six MCM subunits (6×KA). Fig. 6*B* shows that the 6×KA complex is completely unable to bind ssDNA, indicating that either the MCM Walker A mutations block nucleotide binding rather than hydrolysis or, alternatively, prevent the effects of ATP binding from being transmitted to the DNA-binding domain(s). In contrast, the other MCM complexes demonstrate a range of ssDNA binding activities. The complex containing the MCM4KA mutation is completely devoid of ATP-stimulated ssDNA binding; complexes containing the mutation in MCM2 or MCM6 bind ssDNA at essentially wild type levels; and complexes with mutations in MCM3, MCM5, or MCM7 demonstrate intermediate levels of binding.

The ssDNA binding activity of these complexes was further explored by measuring their nucleotide dependence (Fig. 6*C*). In most cases, ssDNA binding is stimulated by both ATP and ATPγS in a manner similar to the wild type MCM2–7 complex. However, we have repeatedly noticed that the MCM2–7 preparations containing the MCM7KA mutation demonstrate elevated levels of ATP-independent ssDNA binding; this binding is only stimulated slightly by ATPγS but not by ATP. The significance of this observation is currently unknown. Nevertheless, these results indicate that unlike steady-state ATP hydrolysis (17), participation of the six MCM ATPase active sites in ssDNA binding is very different, with only the MCM4 subunit, and to a smaller extent the MCM7 subunit, being key to this activity.

The Difference in ssDNA Association Rates between MCM2–7 and MCM467 Depends upon the MCM2/5 Active Site—MCM2–7 contains three MCM subunits that MCM467 lacks: MCM2, 3, and 5. Because the MCM2–7 and MCM467 complexes differ in their association rate with ssDNA, the MCM2, 3, or 5 subunits

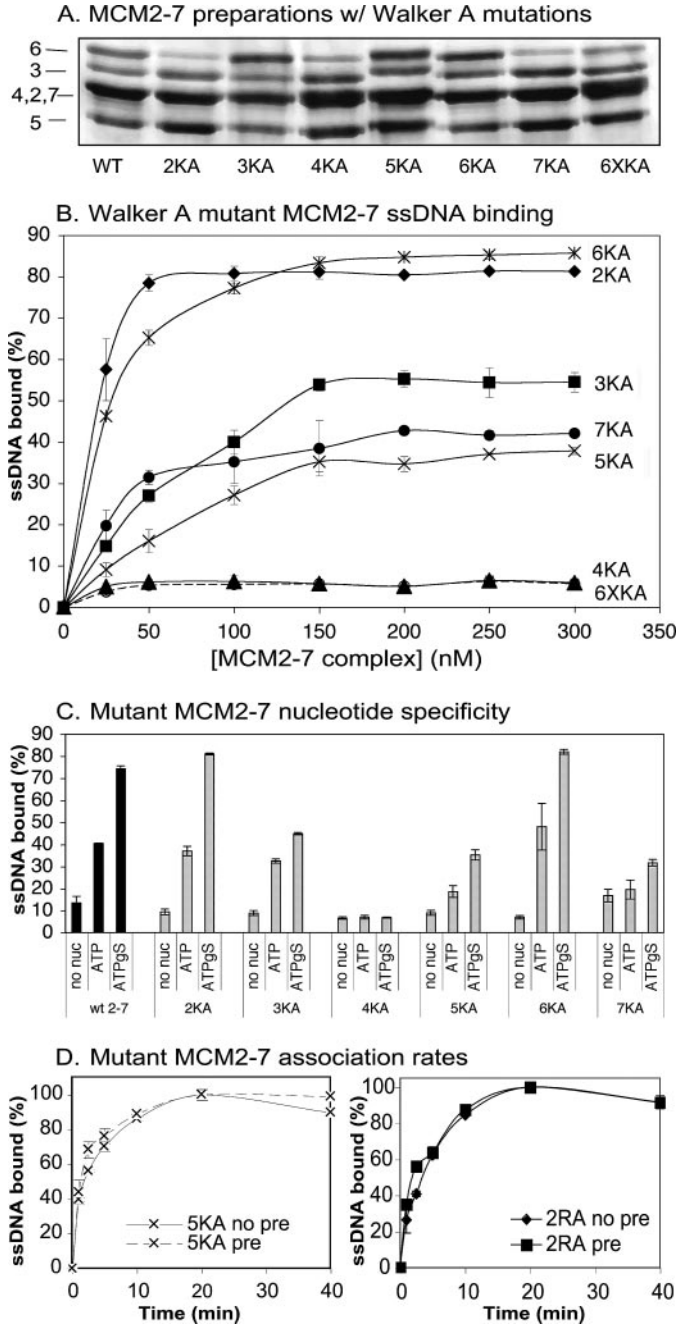

FIGURE 6. **Effect of Walker A substitution mutations on MCM2–7·ssDNA binding.** *A*, SDS-PAGE gel of 2 pmol each of the indicated MCM2–7 preparations following silver staining. *B*, titrations of mutant MCM2–7 complexes for ssDNA filter binding experiments. These experiments are identical to those in Fig. 2*A*, except that each MCM2–7 preparation contained a KA mutation in the indicated subunit, whereas the remaining five subunits are wild type (*WT*). The 6×KA preparation contains the Walker A mutation in all six subunits. The reactions used 4 nM radiolabeled oligonucleotide 510 (supplemental Table S1) in the presence of 5 mM ATPγS. *C*, nucleotide stimulation of ssDNA binding by the KA mutant MCM2–7 preparations. The indicated binding reactions either contained no nucleotide (*no nuc*), 5 mM ATP, or 5 mM ATPγS (*ATPgS*) with 4 nM oligonucleotide 510 and 120 nm of mutant complex. *D*, mutant MCM/ssDNA association kinetics. The association plots for MCM5KA (*left*) and MCM2RA (*right*) hexamers are shown. These experiments were conducted the same as in Fig. 5*A* (*no pre*) and Fig. 5*B* (*pre*).

are likely to be involved in this effect. Knowing that preincubation with ATP relieves the difference in ssDNA association rates between MCM2–7 and MCM467, we reasoned that a mutation in the ATPase active site of MCM2, 3, or 5 may alter the ssDNA association rate of MCM2–7. Of the KA mutant MCM complexes that still demonstrate ATP-dependent ssDNA binding, association kinetics were measured with and without ATP preincubation. Complexes that contain KA mutations in MCM2, 3, or 6 give results similar to the wild type MCM2–7 complex; in these cases, preincubation of the complex with ATP increases the association rate to MCM467 levels (supplemental Fig. S3). In sharp contrast, a MCM2–7 complex containing the MCM5 Walker A mutation binds ssDNA at a similar fast rate in both the presence and absence of ATP preincubation (Fig. 6*D*, *left panel*). This indicates that the MCM5 ATP active site is uniquely involved in the slow ATP-dependent step in MCM2–7 ssDNA association.

The MCMs, like most AAA^+ ATPases, form ATP active sites at subunit interfaces; one subunit contributes a Walker A motif, whereas the adjacent subunit contributes an essential arginine (41). The MCM5 Walker A motif is predicted to form an active site with the essential arginine of MCM2 (41). To test the involvement of MCM2 in the MCM2–7 association rate, we generated MCM2–7 complexes with appropriate arginine to alanine substitutions (R→A)[5] and assayed their association rates. Strikingly, only the MCM2–7 complex containing the MCM2RA mutation demonstrated an accelerated ssDNA association rate (data not shown and Fig. 6*D*, *right panel*). This result further substantiates the involvement of the MCM2/5 active site in MCM2–7 ssDNA association.

DISCUSSION

Our comparative analysis of the ssDNA binding properties of the MCM2–7 and MCM467 complexes reveals similarities and key functional differences both between these complexes and in relation to other helicases. In common with typical hexameric helicases, both MCM complexes demonstrate (pseudo)6-fold symmetry and ATP-dependent ssDNA binding. However, unlike typical homohexameric helicases that contain functionally equal subunits and bind ssDNA in a sequence-independent manner, our data indicate that the MCM2–7 subunits have differential involvement in ssDNA binding and a marked binding preference for poly(dT). Although both complexes have similar ssDNA binding affinities, they differ in their ssDNA association kinetics, evidence suggesting that the MCM2, 3, and 5 subunits regulate the loading or activation of the MCM2–7 complex *in vivo*. Further, our data demonstrate that the lack of helicase activity by the MCM2–7 complex is not due to an inability to bind ssDNA, as previously suggested (41).

The MCM Complex Has Unusual Properties for a Hexameric Helicase—Although helicases usually bind ssDNA in a sequence-independent manner (2), the MCMs prefer to bind to polypyrimidine tracts. Although this property was previously observed for MCM467 (14, 18), we show that this preference is even stronger with MCM2–7 (Fig. 3*A*). Because eukaryotic replication origins are usually A/T-rich (42–44) and often contain poly(dT) tracts (45, 46), an increased affinity to poly(dT) sequences could facilitate loading of the MCMs onto replication origins as previously proposed (18). However, this

[5] M. Bochman, S. Bell, and A. Schwacha, manuscript in preparation.

enhanced affinity for poly(dT) is also potentially disruptive during elongation *in vivo*; helicases need to freely translocate along DNA, and a high affinity toward poly(dT) might impede translocation and cause the replication fork to pause. Such events are deleterious; pausing leads to fork collapse and the production of potentially lethal DNA double strand breaks (47). Possible fork pausing by the MCM complex during normal replication may have broader implications for human health, because DNA replication in eukaryotes sometimes pathologically results in chromosome breaks at A/T-rich sequences referred to as fragile sites (reviewed in Ref. 48).

In contrast to homohexameric helicases, the individual MCM subunits contribute differentially to ssDNA binding. Analysis of MCM2–7 complexes containing Walker A mutant subunits reveals that, unexpectedly, only the active site on MCM4 is absolutely required for this activity, whereas the MCM7 active site is required to make the interaction ATP-dependent. Previous analysis supports these observations. In *Schizosaccharomyces pombe*, MCM complexes containing the MCM4KA mutation lose association with chromatin (19). In contrast, MCM6KA mutant complexes can still bind chromatin in a semi-purified *Xenopus in vitro* DNA replication system (15, 49). One puzzling feature of the MCM2–7 complex is why it contains six distinct subunits. Our data suggest this arrangement has allowed individual subunits to evolve specialized functions, with some subunits specializing in ssDNA binding (MCM4 and 7), whereas other subunits may specialize in regulating this association (MCM2 and 5, below).

Key Differences between the Two MCM Complexes—Both the archaeal MCM complex (12, 50–53) and the eukaryotic MCM467 complex (39, 53) bind dsDNA. This ability has fueled speculation that MCM2–7 might function as a dsDNA pump (54). Although we demonstrate that both complexes have an ATP-dependent dsDNA binding activity, their affinity for dsDNA is ~100-fold lower than for ssDNA. Because MCM467 binds dsDNA better than MCM2–7, it suggests that the MCM2, 3, or 5 subunits may negatively affect dsDNA binding, raising the possibility that regulation of these subunits may facilitate dsDNA interaction under certain conditions. The poor affinity of MCM2–7 for dsDNA does not definitively rule out its involvement as a pump, however. Further mutational analysis of the MCM complex using mutants that specifically affect dsDNA binding (as have been developed in the archaeal MCM complex (12)) will be required to determine the *in vivo* significance of dsDNA binding.

Unexpectedly, MCM2–7 and MCM467 bind ssDNA with different kinetics. Although the MCM467 complex binds ssDNA relatively quickly, MCM2–7 binds approximately five times more slowly. The slow ssDNA association by MCM2–7 is due to an interaction involving ATP, because preincubation of the MCM2–7 complex with ATP removes this kinetic barrier. The effects of preincubation occur very slowly, requiring about 20–25 min of MCM/ATP preincubation to stimulate maximal ssDNA binding (data not shown). This slow rate does not reflect slow ATP binding to the complex, because no noticeable time lag was observed in steady-state ATPase hydrolysis studies of the MCM2–7 complex.[6] We hypothesize that the slow step corresponds to an ATP-dependent conformational change by the MCM2–7 complex. Because the obvious differences between these two complexes are the MCM2, 3, and 5 subunits, it is reasonable to expect that these subunits are responsible for the difference in ssDNA association. This expectation is confirmed by our finding that the MCM5KA and MCM2RA mutant complexes bind ssDNA quickly without ATP preincubation, implying the involvement of these subunits in this slow ssDNA association step.

The Possible Nature of the MCM2–7 ATP-dependent Conformational Change—As previously demonstrated (16), the ATP active sites within the MCM complex lay at dimer interfaces, with one subunit contributing a Walker A motif, whereas the other subunit contributes a catalytically essential arginine "finger." This arrangement is typical for AAA^+ ATPases (reviewed in Ref. 55). To fit these subunit associations onto the observed toroidal structure, MCM2 and MCM5 need to be juxtaposed to form an active site, with MCM5 contributing the Walker A motif and MCM2 contributing the essential catalytic arginine (16).

The effect of either the MCM5KA or the MCM2RA mutation on the association of MCM2–7 with ssDNA is puzzling. Both motifs likely ablate important contacts with ATP, suggesting that normally the slow association reflects an inhibitory nucleotide, or other possible inhibitor, bound at this site. In contrast, preincubation of MCM2–7 with ATP increases ssDNA association, suggesting that ATP binding is responsible for this effect. We suggest that both situations may serve to displace some inhibitory interaction at the MCM2/5 active site, either of a protein-protein or protein-ligand nature, resulting in a conformational change that increases the ssDNA association rate. One possible inhibitor could be ADP that has remained tightly bound to this site during protein purification, a common property of ATPases (56, 57).

Is this proposed conformational change at the MCM2/5 interface physiologically relevant? In common with the other MCM genes, *MCM2* and *MCM5* are essential, indicating that the MCM467 helicase activity is insufficient to carry out *in vivo* DNA replication. Yet our previous analysis indicates that neither MCM2 nor MCM5 has critical involvement in ssDNA binding or steady-state ATP hydrolysis (17), suggesting that their essential *in vivo* function depends upon some yet undiscovered activity.

Available evidence supports a regulatory role for these two subunits in DNA association. Unlike the other five MCM subunits, MCM2 specifically binds chromatin (58). Further, both MCM2 and the MCM5 are linked to the CDC7/DBF4 regulatory kinase, which aids in cell cycle-dependent assembly of the elongation complex and functions immediately downstream of MCM2–7 loading at replication origins (3). Although the mechanistic role of CDC7/DBF4 phosphorylation is poorly understood, the MCM complex is likely to be the focus of its activity. A specific mutant in MCM5 (59) exists that bypasses the normally essential function of CDC7 in DNA replication,

[6] A. Schwacha, unpublished observations.

and the MCM2 subunit is a major substrate for this kinase (60, 61). These results suggest that both MCM2 and MCM5 serve a regulatory function, possibly to activate MCM2–7 helicase activity. Perhaps MCM phosphorylation by the CDC7/DBF4 kinase causes a favorable conformational change at the MCM2/5 site that activates the DNA unwinding activity of the MCM2–7 complex *in vivo*.

Acknowledgments—We thank Robert Duda and James Conway for assistance with electron microscopy and image reconstruction and Lisa Engler and Linda Jen-Jacobson for advice on DNA filter binding and rate measurements. We also thank Steve Bell, Jeff Brodsky, Linda Jen-Jacobson, Julia van Kessel, and members of the Schwacha lab for comments on this manuscript.

REFERENCES

1. Kawasaki, Y., and Sugino, A. (2001) *Mol. Cells* **12,** 277–285
2. Patel, S. S., and Picha, K. M. (2000) *Annu. Rev. Biochem.* **69,** 651–697
3. Bell, S. P., and Dutta, A. (2002) *Annu. Rev. Biochem.* **71,** 333–374
4. Messer, W. (2002) *FEMS Microbiol. Rev.* **26,** 355–374
5. Myllykallio, H., and Forterre, P. (2000) *Trends Microbiol.* **8,** 537–539
6. Forsburg, S. L. (2004) *Microbiol. Mol. Biol. Rev.* **68,** 109–131
7. Koonin, E. V. (1993) *Nucleic Acids Res.* **21,** 2541–2547
8. McMacken, R., Silver, L., and Georgopoulos, C. (1987) *Escherichia coli and Salmonella typhimirium*, pp. 564–612, American Society for Microbiology, Washington, DC
9. Chong, J. P., Hayashi, M. K., Simon, M. N., Xu, R. M., and Stillman, B. (2000) *Proc. Natl. Acad. Sci. U. S. A.* **97,** 1530–1535
10. Kelman, Z., Lee, J. K., and Hurwitz, J. (1999) *Proc. Natl. Acad. Sci. U. S. A.* **96,** 14783–14788
11. Shechter, D. F., Ying, C. Y., and Gautier, J. (2000) *J. Biol. Chem.* **275,** 15049–15059
12. Pucci, B., De Felice, M., Rossi, M., Onesti, S., and Pisani, F. M. (2004) *J. Biol. Chem.* **279,** 49222–49228
13. Ishimi, Y. (1997) *J. Biol. Chem.* **272,** 24508–24513
14. Lee, J. K., and Hurwitz, J. (2001) *Proc. Natl. Acad. Sci. U. S. A.* **98,** 54–59
15. You, Z., Komamura, Y., and Ishimi, Y. (1999) *Mol. Cell. Biol.* **19,** 8003–8015
16. Davey, M. J., Indiani, C., and O'Donnell, M. (2003) *J. Biol. Chem.* **278,** 4491–4499
17. Schwacha, A., and Bell, S. P. (2001) *Mol. Cell* **8,** 1093–1104
18. You, Z., Ishimi, Y., Mizuno, T., Sugasawa, K., Hanaoka, F., and Masai, H. (2003) *EMBO J.* **22,** 6148–6160
19. Gomez, E. B., Catlett, M. G., and Forsburg, S. L. (2002) *Genetics* **160,** 1305–1318
20. Aparicio, T., Ibarra, A., and Mendez, J. (2006) *Cell Div.* **1,** 18
21. Kaplan, D. L., Davey, M. J., and O'Donnell, M. (2003) *J. Biol. Chem.* **278,** 49171–49182
22. Wong, I., and Lohman, T. M. (1993) *Proc. Natl. Acad. Sci. U. S. A.* **90,** 5428–5432
23. Riggs, A. D., Bourgeois, S., and Cohn, M. (1970) *J. Mol. Biol.* **53,** 401–417
24. Winter, R. B., Berg, O. G., and von Hippel, P. H. (1981) *Biochemistry* **20,** 6961–6977
25. Adachi, Y., Usukura, J., and Yanagida, M. (1997) *Genes Cells* **2,** 467–479
26. Sato, M., Gotow, T., You, Z., Komamura-Kohno, Y., Uchiyama, Y., Yabuta, N., Nojima, H., and Ishimi, Y. (2000) *J. Mol. Biol.* **300,** 421–431
27. Yabuta, N., Kajimura, N., Mayanagi, K., Sato, M., Gotow, T., Uchiyama, Y., Ishimi, Y., and Nojima, H. (2003) *Genes Cells* **8,** 413–421
28. Pape, T., Meka, H., Chen, S., Vicentini, G., van Heel, M., and Onesti, S. (2003) *EMBO Rep.* **4,** 1079–1083
29. Chen, Y. J., Yu, X., Kasiviswanathan, R., Shin, J. H., Kelman, Z., and Egelman, E. H. (2005) *J. Mol. Biol.* **346,** 389–394
30. Costa, A., Pape, T., van Heel, M., Brick, P., Patwardhan, A., and Onesti, S. (2006) *J. Struct. Biol.* **156,** 210–219
31. You, Z., and Masai, H. (2005) *Nucleic Acids Res.* **33,** 3033–3047
32. Claycomb, J. M., MacAlpine, D. M., Evans, J. G., Bell, S. P., and Orr-Weaver, T. L. (2002) *J. Cell Biol.* **159,** 225–236
33. Barry, E. R., McGeoch, A. T., Kelman, Z., and Bell, S. D. (2007) *Nucleic Acids Res.* **35,** 988–998
34. Traut, T. W. (1994) *Mol. Cell Biochem.* **140,** 1–22
35. Coue, M., Amariglio, F., Maiorano, D., Bocquet, S., and Mechali, M. (1998) *Exp. Cell Res.* **245,** 282–289
36. Edwards, M. C., Tutter, A. V., Cvetic, C., Gilbert, C. H., Prokhorova, T. A., and Walter, J. C. (2002) *J. Biol. Chem.* **277,** 33049–33057
37. Shin, J. H., and Kelman, Z. (2006) *J. Biol. Chem.* **281,** 26914–26921
38. Saenger, W. (1984) *Principles of Nucleic Acid Structure*, page 310, Springer-Verlag, New York
39. Kaplan, D. L., and O'Donnell, M. (2004) *Mol. Cell* **15,** 453–465
40. Picha, K. M., Ahnert, P., and Patel, S. S. (2000) *Biochemistry* **39,** 6401–6409
41. Davey, M. J., and O'Donnell, M. (2003) *Curr. Biol.* **13,** R594–596
42. Aladjem, M. I., Rodewald, L. W., Kolman, J. L., and Wahl, G. M. (1998) *Science* **281,** 1005–1009
43. Boulikas, T. (1996) *J. Cell. Biochem.* **60,** 297–316
44. Spradling, A. C. (1999) *Genes Dev.* **13,** 2619–2623
45. Okuno, Y., Satoh, H., Sekiguchi, M., and Masukata, H. (1999) *Mol. Cell. Biol.* **19,** 6699–6709
46. Dai, J., Chuang, R. Y., and Kelly, T. J. (2005) *Proc. Natl. Acad. Sci. U. S. A.* **102,** 337–342
47. Cha, R. S., and Kleckner, N. (2002) *Science* **297,** 602–606
48. Arlt, M. F., Casper, A. M., and Glover, T. W. (2003) *Cytogenet Genome Res.* **100,** 92–100
49. Ying, C. Y., and Gautier, J. (2005) *EMBO J.* **24,** 4334–4344
50. Fletcher, R. J., Bishop, B. E., Leon, R. P., Sclafani, R. A., Ogata, C. M., and Chen, X. S. (2003) *Nat. Struct. Biol.* **10,** 160–167
51. Fletcher, R. J., Shen, J., Gomez-Llorente, Y., Martin, C. S., Carazo, J. M., and Chen, X. S. (2005) *J. Biol. Chem.* **280,** 42405–42410
52. Jenkinson, E. R., and Chong, J. P. (2006) *Proc. Natl. Acad. Sci. U. S. A.* **103,** 7613–7618
53. Shin, J. H., Jiang, Y., Grabowski, B., Hurwitz, J., and Kelman, Z. (2003) *J. Biol. Chem.* **278,** 49053–49062
54. Laskey, R. A., and Madine, M. A. (2003) *EMBO Rep.* **4,** 26–30
55. Iyer, L. M., Leipe, D. D., Koonin, E. V., and Aravind, L. (2004) *J. Struct. Biol.* **146,** 11–31
56. Garrett, N. E., and Penefsky, H. S. (1975) *J. Biol. Chem.* **250,** 6640–6647
57. Hackney, D. D. (1988) *Proc. Natl. Acad. Sci. U. S. A.* **85,** 6314–6318
58. Ishimi, Y., Ichinose, S., Omori, A., Sato, K., and Kimura, H. (1996) *J. Biol. Chem.* **271,** 24115–24122
59. Hardy, C. F., Dryga, O., Seematter, S., Pahl, P. M., and Sclafani, R. A. (1997) *Proc. Natl. Acad. Sci. U. S. A.* **94,** 3151–3155
60. Lei, M., Kawasaki, Y., Young, M. R., Kihara, M., Sugino, A., and Tye, B. K. (1997) *Genes Dev.* **11,** 3365–3374
61. Masai, H., and Arai, K. (2000) *Biochem. Biophys. Res. Commun.* **275,** 228–232

DNA binding by the MCM2-7 and MCM467 complexes.

Supplemental data

Supplemental Methods

Co-IPs. MCM subunit association following the final step in purification was verified by co-immunoprecipitation of the complex using AS6.1 (anit-MCM4), followed by verification of individual MCM subunits in the precipitate: 2 pmol of either MCM2-7 or MCM467 were incubated with AS6.1 and 30 µL of 1xPBS-equlibrated GammaBind Plus beads (GE Healthcare) for ≥ 2 hours at 4°C, washed extensively with buffer B2, resuspended in SDS-PAGE loading buffer, and separated by electrophoresis.

Gel filtration chromatography. A 1 ml glass pipet was packed with Sephacryl 300 HR (Sigma) equilibrated in buffer B2 and calibrated with standard molecular weight markers including blue dextran (2,000 kDa), thyroglobulin (669 kDa), apoferritin (443 kDa), β-amylase (200 kDa), and BSA (66 kDa). Small samples of purified protein (20-25 µl, approximately 10 µg) were subjected to analytical gel filtration chromatography run by gravity flow at room temperature. 21 µl fractions were collected and analyzed by SDS-PAGE and staining with Sypro orange.

Two-dimensional gel electrophoresis. Tube gels (6 cm length, 1.3 mm width) were cast in capillary tubes using first-dimension gel solution (8.0 M urea, 4% acrylamide (30% acrylamide:5.4% bis-acrylamide), 2% Triton X-100, 2% high resolution 3/10 ampholyte (Fluka), 0.01% ammonium persulfate, and 0.1% TEMED) and were pre-run for 10 min at 12.5V/cm, 15 min at 19V/cm, and 15 min at 25V/cm. The upper chamber buffer is 200 mM NaOH and the lower chamber buffer is 10 mM H_3PO_4, both thoroughly degassed. MCM protein samples were mixed with equal volumes of first-dimension sample buffer (8.0 M urea, 2% Triton X-100, 5% β-mercaptoethanol, and 2% 3/10 ampholyte) for ≥10 min at room temperature prior to electrophoresis. For isoelectric focusing, samples were loaded directly onto tube gels, overlaid with two volumes of overlay buffer (4.0 M urea, 1% 3/10 ampholyte, 0.01% bromphenol blue), and separated in the first-dimension by electrophoresis for 10 min at 31V/cm and 3.5 hr at 47V/cm. Gels were then extruded from the tubes, equilibrated in SDS-PAGE sample buffer, and proteins separated in the second-dimension on 7% SDS-PAGE gels. Following separation, proteins were either visualized by Sypro orange staining, or transferred to nitrocellulose for Western blot analysis.

Electron Microscopy. Proteins were diluted to 50 µg/ml in buffer B3 supplemented with 5 mM ATPγS. They were then absorbed to glow-discharged, formvar/carbon-coated 400 mesh copper grids (Ted Pella, Redding, CA) and negatively stained with 2% uranyl acetate. Grids were visualized with an FEI Morgagni 286 transmission electron microscope at 80 kV and 56,000X (wide field) or 140,000X (individual particle) magnification. Micrographs were taken with an AMT digital camera (Peltier-cooled Hamamatsu ORCA-HR CCD camera) at a resolution of 2624x2624 pixels. Quantification and classification of MCM complexes were done semi-automatically by selecting single particles from micrographs with BOXER (http://ncmi.bcm.tmc.edu/~stevel/EMAN/doc/) using reference particles of each class (random orientation, toroidal, split-ring). Particles were then manually categorized. Image averaging was performed as described (1). In brief, representative images were chosen from the dataset of selected particles, and an image with good contrast was used as the initial reference in each case. The image was low-pass filtered to remove very high-frequency noise, and all selected particles were correlation-aligned by an exhaustive search in 6° steps over the in-plane rotation angle, and within a radius of 10 pixels for the origin. The best-scoring 50% of the particles were combined to make a new reference model, and a subsequent refinement of orientation parameters was carried out in finer steps over a limited rotation range and translational offset.

Measurement of MCM/ssDNA dissociation kinetics. To measure dissociation, the standard MCM/ssDNA binding reaction was scaled up 10-fold, and protein/ssDNA complexes were allowed to form for 30 minutes at 30°C. Then, a 1000-fold molar excess of unlabelled oligo 510 (Supplemental Table 1) was

added (t = 0), and samples were withdrawn at the indicated intervals and assayed by filter binding. The dissociation kinetics were plotted as described (2) where (RO) represents the concentration of MCM/ssDNA complex at time t and $(RO)_o$ is the concentration of MCM/ssDNA complex at t = 0.

Quantitative western blots. Known amounts of MCM hexamer and single subunit preparations were separated by SDS-PAGE, transferred to a nitrocellulose membrane, and analyzed by western blotting using subunit-specific antibodies: Santa Cruz anti-MCM2 (sc-6680) or anti-MCM7 (sc-6688). The corresponding chemiluminescent signal was quantified prior to signal saturation using an LAS-3000 Intelligent Dark Box (Fujifilm) and Image Gauge software. The amount of MCM2 or MCM7 in the hexamer was calculated using the single subunit titrations as standard curves.

Supplemental References

1. Ross, P. D., Conway, J. F., Cheng, N., Dierkes, L., Firek, B. A., Hendrix, R. W., Steven, A. C., and Duda, R. L. (2006) *J Mol Biol* **364**(3), 512-525
2. Riggs, A. D., Bourgeois, S., and Cohn, M. (1970) *J Mol Biol* **53**(3), 401-417

DNA binding by the MCM2-7 and MCM467 complexes.

Supplemental Table 1. Oligonucleotides used (* denotes sites of biotinylation).

Oligo # (length)	Sequence (5'→3')
233 (85 nt)	TTTTTTTTTTTTTTTTTTTTTTTTTTTTTTTTTTTTTTTTTGGTTGGCCGATCAAGT GCCCAGTCACGACGTTGTAAAACGAGCCC
235 (90 nt)	CACTCGGGCTCGTTTTACAACGTCGTGACTGGGCACTTGATCGGCCAACCTT TTTTTTTTTTTTTTTTTTTTTTTTTTTTTTTTTT
510 (85 nt)	ACCTGTCGTGCCAGCTGCATTAATGAATCGACTGCTCTCACATATAGCTACA TATCCGACGCGACCACTCACAATCACAGTTAAC
455 (90 nt)	*GGGCTCGTTTTACAACGTCGTGACTGGGCACTTGATCGGCCAACCTTTTTTT TTTTTTTTTTTTTTTTTTTTTTTTTTTTTTTTTT
3 (44 nt)	GGTGTTTGTTGTATTAACCAGTTTGATAAAATGAGTGATTCTAC
806 (23nt)	GTTAACTGTGATTGTGAGTGGTC
770 (15 nt)	TTTTTTTTTTTTTTT
771 (20 nt)	TTTTTTTTTTTTTTTTTTTT
772 (25 nt)	TTTTTTTTTTTTTTTTTTTTTTTTT
773 (30 nt)	TTTTTTTTTTTTTTTTTTTTTTTTTTTTTT
774 (35 nt)	TTTTTTTTTTTTTTTTTTTTTTTTTTTTTTTTTTT
775 (40 nt)	TTTTTTTTTTTTTTTTTTTTTTTTTTTTTTTTTTTTTTTT
776 (50 nt)	TTTTTTTTTTTTTTTTTTTTTTTTTTTTTTTTTTTTTTTTTTTTTTTTTT
777 (60 nt)	TTTTTTTTTTTTTTTTTTTTTTTTTTTTTTTTTTTTTTTTTTTTTTTTTTTTTTTTT TT
778 (80 nt)	TTTTTTTTTTTTTTTTTTTTTTTTTTTTTTTTTTTTTTTTTTTTTTTTTTTTTTTTT TTTTTTTTTTTTTTTTTTTT

DNA binding by the MCM2-7 and MCM467 complexes.

Supplemental Table 2. MCM physical constants determined in this study*

Physical constant	MCM2-7	MCM467
Single-stranded DNA interactions:		
K_d as a function of [MCM], ATP	38.0±8.5 nM	50.0±18.2 nM
K_d as a function of [MCM], ATPγS	32.8±4.3 nM	23.5±4.7 nM
K_d as a function of [ssDNA], ATP	43.6±9.7 nM	18.4±5.9 nM
K_d from EMSA, ATPγS	N.A.	~40 nM
$k_{a\ (apparent)}$, ATPγS (no pre-inc)	$4.22x10^5$ $M^{-1}min^{-1}$	$1.82x10^6$ $M^{-1}min^{-1}$
$k_{a\ (apparent)}$, ATPγS (pre-inc)	$2.28x10^6$ $M^{-1}min^{-1}$	$1.69x10^6$ $M^{-1}min^{-1}$
$k_{d,slow}$, ATPγS	0.0068 min^{-1}	0.002 min^{-1}
$k_{d,fast}$, ATPγS	0.0407 min^{-1}	0.0241 min^{-1}
K_d calculated from rate constants	17.8 nM	14.3 nM
Double-stranded DNA interactions:		
K_d as a function of [dsDNA], ATPγS	2.1±0.2 μM	5.60±0.6 μM

* These physical constants are not corrected for the ssDNA binding specific activity of our preparations, which average about 50% (See Supplemental Figure 1).

DNA binding by the MCM2-7 and MCM467 complexes.

Supplemental Figure Legends

Supplemental Figure 1. *Characterization of purified MCM2-7 and MCM467 complexes*. A.) SDS-PAGE and profile tracing of 3 pmol of representative MCM2-7 and MCM467 preparations. The identity of the MCM subunits is as noted. The MCM2, 4, and 7 subunits are of similar size and do not resolve. B.) Co-immunoprecipitation of MCM subunits from the final preparations. Western blots were used to verify that the co-migrating subunits in either the MCM2-7 (MCM2, 4, and 7) or MCM467 (MCM4 and 7) preparations. The same blot was stripped and re-probed for each Western. C) Gel filtration of final MCM preparations. Preparations of MCM2-7, MCM467, and a single subunit preparation of MCM3 as separated by gel filtration and the indicated fractions analyzed by SDS-PAGE. The calculated size of both the MCM2-7 and MCM467 hexamer is ~600 kDa, while that of the MCM3 monomer is ~107 kDa**.** These data are consistent with our previous observation that MCM2-7 runs at about 800 kDa and MCM3 runs at about 200 kDa by gel filtration (Schwacha and Bell, 2001). D) Two-dimensional electrophoresis of final MCM preparations. Sypro orange stained gels are shown for MCM2-7 (left) and MCM467 (right). Indicated position of individual MCM subunits were established by Western blotting using MCM subunit-specific antibodies. Note that MCM2 and MCM7 could not be resolved by this approach. For MCM467, the ratio of MCM4:6:7 was 1.9:1:1.2, with MCM6 being the least abundant subunit. Among various MCM467 preparations used in this study, our quantitation suggests that up to 50-78% of the complexes have a 1:1:1 subunit stoichiometry. E) Examining the specific activity of ssDNA binding by our MCM2-7 and MCM467 preparations. ssDNA binding conditions are similar to that listed in Materials and Methods, except 100 nM of radiolabeled oligo 510 was used and ATPγS was present to 5 mM. ssDNA binding by the indicated amounts of MCM2-7 or MCM467 preparations are shown. Note: for technical reasons and difficulty of obtaining sufficient quantities, we are unable to conduct this binding experiment at sufficiently high reactant concentrations to accurately assess specific activity. Under the current conditions, the ratio of protein:DNA at each point represents the lower limit of specific activity. From this graph, 50% ssDNA binding of MCM2-7 or MCM467 corresponds to approximately 60% and 40%, of the calculated hexamers in these preparations, which we take as the minimal specific ssDNA binding activity. F) Quantitative Westerns to measure the amount of MCM2 and MCM7 in MCM2-7 preparations. Indicated amounts of the final MCM2-7 preparations and purified MCM2 (left) or purified MCM7 (right) were separated by SDS-PAGE, and quantified by Western Blotting using subunit-specific antibodies. These data, in combination with the two dimensional gels in D), indicate that MCM2 is the limiting subunit in these preparations. In the preparation shown, we calculate that relative to the purified MCM2 standard, that one μg of MCM2-7 complex contains 0.08 μg MCM2. This is consistent with 48% of the MCM2-7 complexes containing all 6 MCM subunits in a 1:1:1:1:1:1 stoichiometry. Conclusion. Among the various MCM2-7 and MCM467 preparations used in this study, our data suggests that approximately 50% of the MCM complexes in these preparations contain an equal subunit stoichiometry and roughly the same fraction is ssDNA binding competent. We however cannot exclude the possibility that a small fraction of the ssDNA binding observed in this paper emanates from MCM subcomplexes, possibly pentamers.

Supplemental Figure 2. *Kinetics of MCM/ssDNA dissociation*. The data for each set was normalized to a maximal ssDNA binding of 100%. A.) Dissociation rates of MCM2-7 and MCM467 from ssDNA. Binding conditions used 5 mM ATPγS and radiolabeled oligo 510 (Supplemental Table 1). B) The data in A as a semi-log plot; slope = k_d. Plotting these data on a semi-log scale reveals that both complexes dissociate in a similar biphasic manner, with a relatively fast initial off-rate, followed by a much slower dissociation (Figure 5B; MCM467 $k_{d,fast}$ = 0.0241 min^{-1}, MCM467 $k_{d,slow}$ = 0.002 min^{-1}, MCM2-7 $k_{d,fast}$ = 0.0407 min^{-1}, MCM2-7 $k_{d,slow}$ = 0.0068 min^{-1}) . The biphasic nature of the plot suggests binding heterogeneity. Although in principle our ssDNA probes are long enough to facilitate cooperative binding of two MCM complexes, repeats of these experiments using a shorter probe that should only allow binding of a single MCM complex (oligo 3, Supplemental Table 1) produced a similar biphasic dissociation (data not shown). In addition, treating our complexes with lambda phosphatase to generate a

uniform population of unphosphorylated MCM complexes also did not affect these results (data not shown).

Supplemental Figure 3. Association of MCM2-7 complexes containing either the A)MCM2K, B) MCM3KA, or C) MCM6KA mutant subunit. Assays were performed as in Figure 5A.

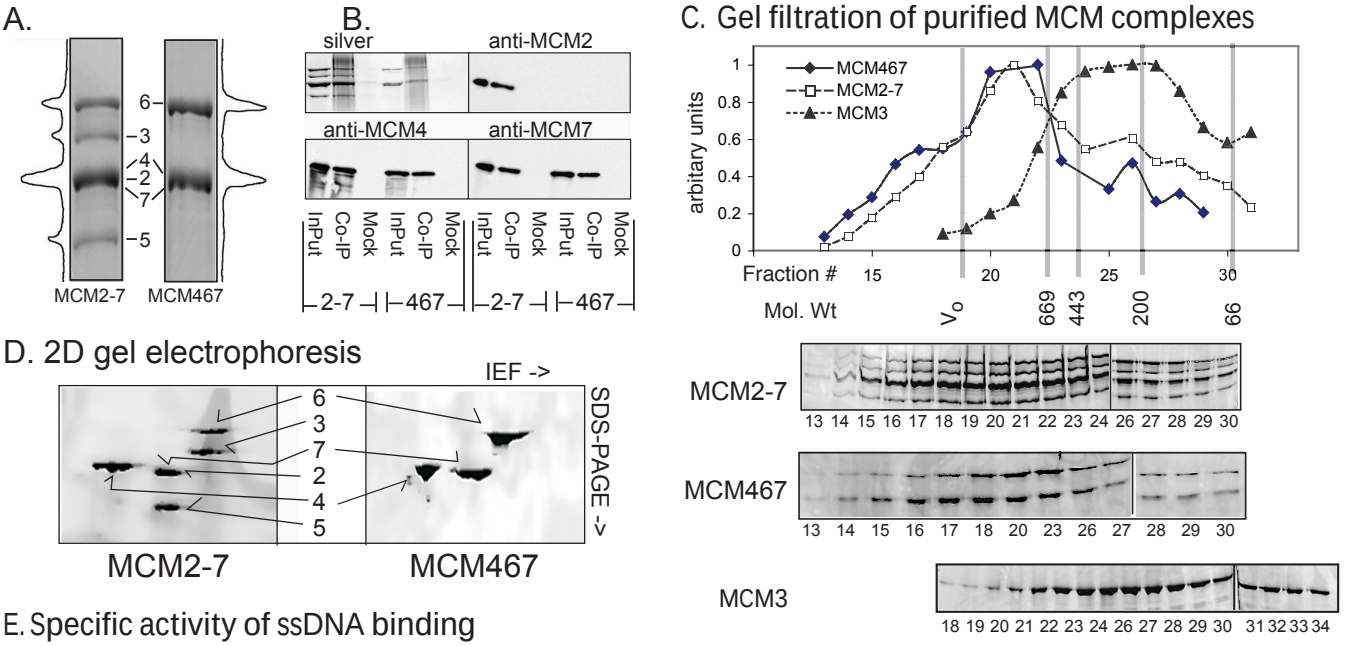

Supplemental Figure 1 082807

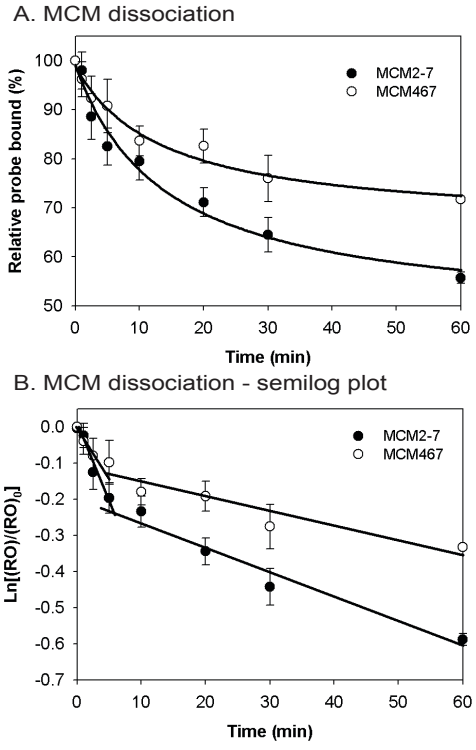

Supplemental Figure 2 04/20/07

A. Association rate MCM2-7 2KA

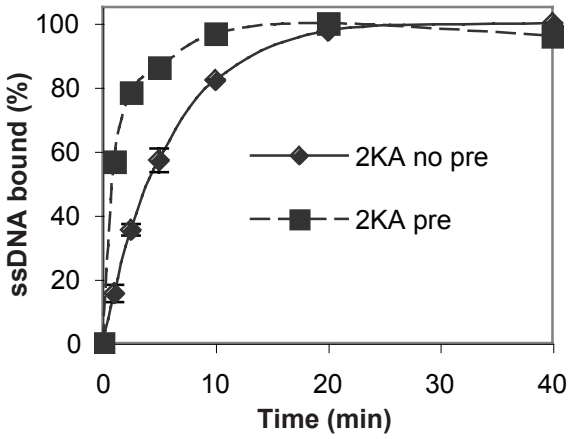

B. Association rate MCM2-7 3KA

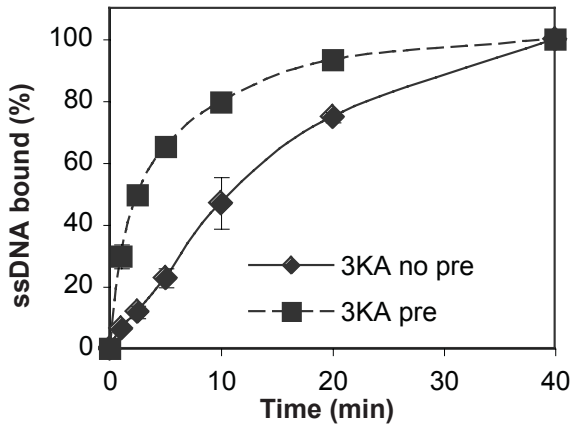

C. Association rate MCM2-7 6KA

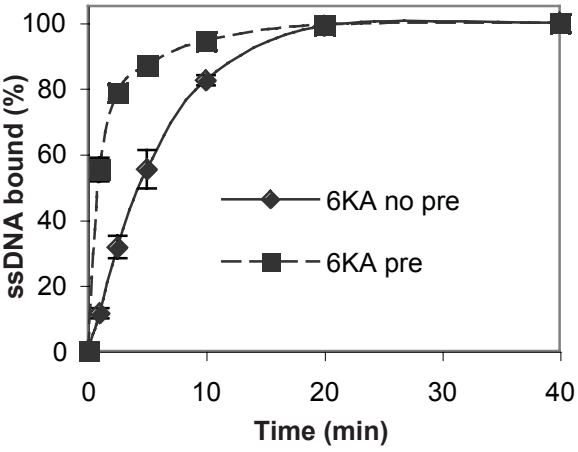

Supplemental Figure 3 08/27/07

Differences in the Single-stranded DNA Binding Activities of MCM2-7 and MCM467: MCM2 AND MCM5 DEFINE A SLOW ATP-DEPENDENT STEP

Matthew L. Bochman and Anthony Schwacha

J. Biol. Chem. 2007, 282:33795-33804.
doi: 10.1074/jbc.M703824200 originally published online September 25, 2007
